PERGAMON

International Journal of Multiphase Flow 26 (2000) 1469–1491

International Journal of Multiphase Flow

www.elsevier.com/locate/ijmulflow

# Steady flow and interfacial shapes of a highly viscous dispersed phase

Runyuan Bai*, Daniel D. Joseph

*Department of Aerospace Engineering and Mechanics, University of Minnesota, Minneapolis, MN 55455, USA*

Received 21 December 1998; received in revised form 27 July 1999

**Abstract**

A perturbation theory for the steady flow of immiscible liquids is developed when the dispersed phase is much more viscous than the continuous phase, as is the case in emulsions of highly viscous bitumen in water and in water lubricated pipelines of heavy crude. The perturbation is nonsingular, but nonstandard; the partitioning of the boundary conditions at different orders is not conventional. At zero-th order the dispersed phase moves as a rigid solid with an as yet unknown, to-be-determined, pressure. The flow of the continuous phase at zero-th order is determined by a Dirichlet problem with prescribed velocities on a to-be-iterated interfacial boundary. The first order problem in the dispersed phase is determined from the solution of a Stokes flow problem driven by the previously determined shear strain on the as yet undetermined interfacial boundary. This Stokes problem determines the unknown, to-be-determined, lowest order pressure distribution. At this point we have enough information to test the balance of normal stresses at lowest order; by iterating the interface shapes we may now complete the description of the lowest order problems. The perturbation sequence in powers of the viscosity ratio has a similar structure at every order and all the problems may be solved sequentially with the caveat that interface shape must be determined iteratively in each perturbation loop.

A perturbation solution for the wavy interfacial shapes on core-annular flows of very viscous oil is presented and the results are compared with experiments and a simpler approximation in which the core moves as rigid, but deformable body with no secondary motions. The perturbation theory gives rise to an accurate description of the bamboo waves observed in experiments when the holdup ratio measured in the experiments is assumed in the theoretical calculation. The perturbation solution and the rigid body approximation are in a relatively good agreement with errors of the order 10% in the flow curves and wave shapes; the error is associated with the neglect of the secondary motion in the rigid-deformable core approximation. 

* Corresponding author.

0301-9322/00/$ - see front matter 
PII: S0301-9322(99)00093-2

## 1. Introduction

Water-lubricated transport of heavy viscous oils is a technology based on a gift of nature in which the water migrates into the region of high shear at the wall of the pipe where it lubricates the flow. Since the pumping pressures are balanced by wall shear stresses in the water, the lubricated flows require pressures comparable to pumping water alone at the same throughput, independent of the viscosity of the oil (if it is large enough). Hence savings of the order of the oil-to-water viscosity ratio can be achieved in lubricated flows. Lubricated flow in an oil core is called core-annular flow, CAF for short.

Typically, waves appear on the surface of the oil core and they appear to be necessary for levitation of the core off the wall when the densities are different and for centering the core when the densities are matched. We call these flows wavy core-annular flow (WCAF). Perfect core-annular flows (PCAF) of density matched fluids in horizontal pipes and, generally in vertical pipes, are possible but are rarely stable (Preziosi et al., 1989; Chen et al., 1990; Joseph and Renardy, 1993).

The science behind the technology of CAF has given rise to a large literature which has been reviewed by Oliemans and Ooms (1986) and more recently by Joseph and Renardy (1993). This literature has many facets, which include models for levitation, empirical studies of energy efficiency of different flow types, empirical correlations giving the pressure drop versus mass flux, stability studies and reports of industrial experience.

Water lubricated pipelining of viscous materials like heavy crude oil is robustly stable and has a high economics potential. Heavy crudes are very viscous and usually are somewhat lighter than water, though crudes heavier than water are not unusual. Typical crudes might have a viscosity of 1000 P and a density of 0.99 g/cm$^3$ at 25°C. Light oils with viscosities less than 5 P do not give rise to stable lubricated flows unless they are processed into water/oil emulsions and stiffened.

An important series of experiments on water lubricated pipelining were carried out in Alberta, Canada by Russell and Charles (1959); Russell et al. (1959) and Charles (1963) and especially by Charles et al. (1961). Glass (1961) found among other things that the lowest pressure gradients were achieved when the water input rate was between 30 and 40%. Other experiments on water lubrication in horizontal pipes we reported by Stein (1978) and Oliemans et al. (1985). Arney et al. (1993) introduced and evaluated a correlation formula which estimated the holdup fraction and friction factor for all available experimental data. A simple theory was given which is based on the concentric core-annular flow model and leads to a Reynolds number and friction factor, which reduces a large body of experimental data on to one curve.

Oil companies have had an intermittent interest in the technology of water-lubricated transport of heavy oil since 1904. Isaacs and Speed (1904) in US Patent No. 759,374 were the first to discuss water lubrication of lighter oils which they proposed to stabilize by centripetal acceleration created by rifling the pipe. For stratified flow, Looman (1916) patented a method of conveying oils by passing them over an array of water traps at the bottom of the pipe. An extended history of patents is presented in Joseph and Renardy (1993). The patent history of the subject as it is presently understood starts with the application of Clark and Shapiro (1949) of Socony Vacuum Oil Company who used additives to reduce the density differences between

the oil and water and anionic surfactants to reduce emulsification of water into oil. Clifton and Handley (1958) of Shell Development proposed to prevent the emulsification of oil at pumps by removing the water before pumping the oil and reinjecting it after. In fact, water-in-oil emulsions can be pumped in a sheath of water despite the fact that the viscosity of the emulsion can be orders of magnitude larger than the oil alone. In general, lubricated flows are more effective when the oil is more viscous; the water/oil emulsion is an 'effective' thickened oil whose density is closer to water. Keil (1968) of Exxon patented a CAF process for pumping heavy oils and water-in-oil emulsions, surrounded by water, for fracturing subterranean formations to increase oil and gas production. Ho and Li (1994) of Exxon produced a concentrated water-in-oil emulsion with 7 to 11 times more water than oil, which they successfully transported in CAF.

Syncrude Canada Ltd has undertaken studies of lubricated transport of a bitumen froth which is obtained from processing of oilsands of Alberta for upgrading to Synthetic crude. The oil (bitumen) is extracted from mined oilsands rather than pumped directly from the reservoir. A hot water extraction process is used to separate bitumen as froth from sand and the average composition of the froth is 60, 30 and 10 wt% bitumen, water and solids, respectively. Internal studies led by Neiman (1986) and recent studies at the University of Minnesota by Joseph et al. (in press) have shown that the produced bitumen froth will self lubricate in a pipe flow.

Probably the most important industrial pipeline to date was the 15.2 cm (6 inch) diameter, 38.6 km (24 mile) long Shell line from the North Midway Sunset Reservoir near Bakersfield, California, to the central facilities at Ten Section. The line was run under the supervision of Veet Kruka for 12 years from 1970 until the Ten Section facility was closed. When lubricated by water at a volume flow rate of 30% of the total, the pressure drop varied between 6.2 and 7.58 MPa at a flow rate of 24,000 barrels per day with the larger pressure at a threshold of unacceptability which called for pigging. In the sixth year of operation the fresh water was replaced with water produced at the well site which contained various natural chemicals leached from the reservoir, including sodium metasilicate in minute 0.6 wt% amounts. After that the pressure drop never varied much from the acceptable 6.2 MPa value; the CAF was stable as long as the flow velocity was at least 0.9 m/s. Industrial experience suggests that inertia is necessary for successful CAF. Also Shell Oil has pioneered the development of commercially viable pipelines. Maraven of PVSA (Petroleos de Venezuela Sociedad Autonornia) has placed in operation a 60-km line to transport heavy crudes in the lubricated mode. In general such lubricated lines become attractive when the lighter crudes are expensive or locally in short supply.

A surprising property of core flow is that the flow in a horizontal line will lubricate with the core levitated off the wall even if the core is lighter or heavier than lubricating water. This levitation could not take place without a hydrodynamic lifting action due to waves sculpted on the core surface. In the case of very viscous liquids, the waves are basically standing waves, which are convected with the core as it moves downstream. This picture suggests a lubrication mechanism for the levitation of the core analogous to mechanisms, which levitate loaded slider leavings at low Reynolds numbers. Ooms et al. (1984) and Oliemans and Ooms (1986) gave a semiemperical model of this type and showed that it generated buoyant forces proportional to

the first power of the velocity to balance gravity. In this theory, the shape of the wave must be given as an empirical input.

Consider water lubricated pipelining of crude oil. The oil rises up against the pipe wall because it is lighter than the water. It continues to flow because it is lubricated by waves. However, the conventional mechanisms of lubrication cannot work. The saw tooth waves are like an array of slipper bearings and the stationary oil core is pushed off the top wall by lubrication forces. If velocity were reversed, the core would be sucked into the wall, so the slipper-bearing picture is obligatory if you want levitation.

Obviously the saw tooth waves are unstable since the pressure is highest just where the gap is smallest, so the wave must steepen where it was gentle, and smooth where it was sharp. To get a lift from this kind of wave it appears that we need inertia, as in flying. Liu's (1982) formula for capsule liftoff in a pipeline in which the critical lift off velocity is proportional to the square root of gravity times the density difference is an inertial criterion. It is likely that inertial dynamics is also involved in lubricated oil and slurry lines. At high speeds the core flows may literally 'fly' down the tube. In all of this, the position of the viscous points of stagnation where the pressures are high is of critical importance.

Joseph in Feng et al. (1995) first mentioned that the shape of the wave core from lubrication theory never exists since high pressure in front of wave crests will deepen the shape. Then Bai et al. (1996) confined their attention to the direct numerical simulation of axisymmetric core flows. The shape of the interface and the secondary motions which develop in a 'flying' core flow have a natural explanation in terms of effects of inertia. Less intuitive is the existence of a threshold Reynolds number corresponding to a change in the sign of the pressure force on the core, from suction at Reynolds numbers below the threshold, as in the reversed slipper bearing in which the slipper is sucked to the wall, to compression for Reynolds numbers greater than the threshold as in flying core flow in which the core can be pushed off the wall by stagnation pressure.

In treating the flow of two immiscible liquids with greatly different viscosity, like bitumen and water, certain simplifications arise when more viscous liquid is dispersed and not attached to rigid boundaries. In this case the dispersed phase may move nearly as a rigid body since the forces which arise from the motion of the continuous phases are not great enough to drive large secondary motions in the dispersed phase. The water will move bitumen dispersed in water more or less as a rigid body provided that the bitumen is not anchored at some wall.

Here and henceforward we shall call the dispersed phase oil and the continuous phase water. We search for simplified mathematical descriptions as a perturbation of a rigid motion in the limit in which the ratio of the water viscosity $\mu_w$ to the oil viscosity $\mu_o$

$$\varepsilon = \frac{\mu_w}{\mu_o} \to 0. \tag{1}$$

Since water is located to the wall, drag reductions of the order of the viscosity ratio are possible

$$\mu_o/\mu_w = 10^5. \tag{2}$$

In this paper we will confine our attention to the cases in which interfacial rheology, and Maragnoni effects are neglected. These effects are greatly diminished by the high bulk viscosity of the dispersed phase and in a later work we will look to describe exactly how diminished these effects are. A preliminary version of the results given were presented in a conference proceeding by Joseph and Bai (1999). Generally speaking, our work here is motivated by needs of the heavy oil industry.

## 2. Governing equations

To keep the description simple, we consider the case when the oil is free to move in water as in the case of sedimentation of a single drop of heavier-than-water oil or the core-annular flow studied by Bai et al. (1996).

In steady flow the oil–water interface is given by

$$F(\chi(\varepsilon),\ \varepsilon) = 0, \tag{3}$$

where $\chi(\varepsilon)$ is the position of points on $F = 0$. The unknowns in our problem are

$$\left.\begin{array}{ll} \boldsymbol{u}(\chi,\ \varepsilon),\ \psi(\chi,\ \varepsilon) & \text{in the oil} \\ \boldsymbol{v}(\chi,\ \varepsilon),\phi(\chi,\ \varepsilon) & \text{in the water} \\ \chi(\varepsilon) & \end{array}\right\}, \tag{4}$$

where $\boldsymbol{u}$ and $\boldsymbol{v}$ are velocities and

$$\left.\begin{array}{l} \psi = p_{\mathrm{o}} + \lambda\cdot\chi + \rho_{\mathrm{o}}\boldsymbol{g}\cdot\chi \\ \phi = p_{\mathrm{w}} + \lambda\cdot\chi + \rho_{\mathrm{w}}\boldsymbol{g}\cdot\chi \end{array}\right\} \tag{5}$$

are 'dynamic' pressures, $p$ is pressure and $\lambda$ and $\boldsymbol{g}$ are constant vectors ($\boldsymbol{g}$ is the gravity; $\lambda = \boldsymbol{e}_z\beta$ for the constant part of the pressure gradient which balances the pressure drop in core-annular flow).

The equations of motion in the oil and water are

$$\left.\begin{array}{l} \operatorname{div}\boldsymbol{u} = 0 \\ \rho_{\mathrm{o}}\boldsymbol{u}\cdot\nabla\boldsymbol{u} = -\nabla\psi + \dfrac{\mu_{\mathrm{w}}}{\varepsilon}\nabla^2\boldsymbol{u} \end{array}\right\}, \tag{6}$$

and

$$\left.\begin{array}{l} \operatorname{div}\boldsymbol{v} = 0 \\ \rho_{\mathrm{w}}\boldsymbol{v}\cdot\nabla\boldsymbol{v} = -\nabla\phi + \mu_{\mathrm{w}}\nabla^2\boldsymbol{v} \end{array}\right\}. \tag{7}$$

At the interface $\chi = \chi_{\mathrm{o}}$ the velocity is continuous

$$\boldsymbol{u}(\chi_{\mathrm{o}}) = \boldsymbol{v}(\chi_{\mathrm{o}}) \tag{8}$$

and the kinematic condition on the interface is

$$\boldsymbol{u}(\chi_{\mathrm{o}})\cdot\boldsymbol{n} = \boldsymbol{v}(\chi_{\mathrm{o}})\cdot\boldsymbol{n} = 0, \tag{9}$$

where $\boldsymbol{n}$ is the normal from oil to water. The shear stress is continuous

$$\tau \cdot D[\boldsymbol{u}(\chi) - \varepsilon \boldsymbol{v}(\chi)] \cdot \boldsymbol{n} = 0, \tag{10}$$

where $D[\boldsymbol{u}]$, the rate of strain, is the symmetric part of $\nabla \boldsymbol{u}$ and $\tau$ is a unit tangent vector in the interface, $\tau \cdot \boldsymbol{n} = 0$. The balance of normal stresses can be expressed as

$$-\phi(\chi) + \psi(\chi) - (\rho_w - \rho_o)\boldsymbol{g} \cdot \chi + 2\mu_w \boldsymbol{n} \cdot D[\boldsymbol{v} - \boldsymbol{u}/\varepsilon] \cdot \boldsymbol{n} = 2H(\chi)\sigma, \tag{11}$$

where $H(\chi)$ is the mean curvature and $\sigma$ is interfacial tension.

The boundary conditions apply only to water, since oil is assumed not to touch the boundary. For steady flow the velocity of the boundary at $\chi = \chi_b$ is

$$\boldsymbol{v}(\chi_b) = V. \tag{12}$$

$V$ is the velocity of solid walls in a coordinate system centered on the falling drop or in a coordinate system moving with the average velocity of the core in annular flow.

## 3. Equations when $\varepsilon \to 0$

Assuming now that all functions listed in Eq. (5) are bounded as $\varepsilon \to 0$, we find that

$$\left.\begin{array}{l} \boldsymbol{u}_o(0) = 0, \\ \operatorname{div} \boldsymbol{u}_o = 0, \\ \nabla^2 \boldsymbol{u}_o = 0, \\ \boldsymbol{u}_o(\chi_o) \cdot \boldsymbol{n}_o = 0, \\ \tau_o \cdot D[\boldsymbol{u}_o(\chi_o)] \cdot \boldsymbol{n}_o = 0, \\ \boldsymbol{n}_o \cdot D[\boldsymbol{u}_o(\chi_o)] \cdot \boldsymbol{n}_o = 0. \end{array}\right\}. \tag{13}$$

The function

$$\boldsymbol{u}_o \equiv 0$$

satisfies Eq. (13). Then, in the water we have

$$\left.\begin{array}{l} \operatorname{div} \boldsymbol{v}_o = 0 \\ \rho_w \boldsymbol{v}_o \cdot \nabla \boldsymbol{v}_o = -\nabla \phi_o + \mu_w \nabla^2 \boldsymbol{v}_o \\ \boldsymbol{v}_o(\chi_o) = 0 \\ \boldsymbol{v}_o(\chi_b) = V \end{array}\right\}. \tag{14}$$

Equations (14) are a Dirichlet problem for $\boldsymbol{v}_o(\chi)$ and $\phi_o(\chi)$ which can be solved when the interface $\chi_o$ is given. No condition on $\boldsymbol{v}(\chi)$ arises from the shear stress balance Eq. (10); and shear stress arising from Eq. (13) is acceptable. The idea is to iterate $\chi_o$, using the $\chi_o$ that will reduce Eq. (11) to an identity. To do this iteration, more work is required.

## 4. Perturbation equations at lowest order

Now we develop a solution in powers of $\varepsilon$, to the lowest order

$$\left.\begin{array}{l} \boldsymbol{u}(\chi,\ \varepsilon) = \varepsilon \boldsymbol{u}_1(\chi) \\ \psi(\chi,\ \varepsilon) = \psi_{\mathrm{o}}(\chi) + \varepsilon\psi_1(\chi), \\ \boldsymbol{v}(\chi,\ \varepsilon) = \boldsymbol{v}_{\mathrm{o}}(\chi) + \varepsilon \boldsymbol{v}_1(\chi), \\ \phi(\chi,\ \varepsilon) = \phi_{\mathrm{o}}(\chi) + \varepsilon\phi_1(\chi), \\ \chi(\varepsilon) = \chi_{\mathrm{o}} + \varepsilon\chi_1 \end{array}\right\}. \tag{15}$$

At this interface, we have

$$\boldsymbol{v}(\chi(\varepsilon),\ \varepsilon) = \boldsymbol{v}_{\mathrm{o}}(\chi_{\mathrm{o}}) + \varepsilon \boldsymbol{v}_1(\chi_{\mathrm{o}}) + \varepsilon\chi_1 \cdot \nabla \boldsymbol{v}_{\mathrm{o}}(\chi_{\mathrm{o}}), \tag{16}$$

$$\phi(\chi(\varepsilon),\ \varepsilon) = \phi_{\mathrm{o}}(\chi_{\mathrm{o}}) + \varepsilon\phi_1(\chi_{\mathrm{o}}) + \varepsilon\chi_1 \cdot \nabla\phi_{\mathrm{o}}(\chi_{\mathrm{o}}). \tag{17}$$

Since

$$\boldsymbol{u}(\chi(\varepsilon),\ \varepsilon) = \varepsilon \boldsymbol{u}_1(\chi_{\mathrm{o}}) + \varepsilon^2 \boldsymbol{u}(\chi_{\mathrm{o}}) + \varepsilon^2\chi_1 \cdot \nabla \boldsymbol{u}_1(\chi_{\mathrm{o}}), \tag{18}$$

but

$$\psi(\chi(\varepsilon),\ \varepsilon) = \psi_{\mathrm{o}}(\chi_{\mathrm{o}}) + \varepsilon\psi_1(\chi_{\mathrm{o}}) + \varepsilon\chi_1 \cdot \nabla\psi_{\mathrm{o}}(\chi_{\mathrm{o}}). \tag{19}$$

Moreover, since the shape of drop changes with

$$\left.\begin{array}{l} \boldsymbol{n}(\chi) = \boldsymbol{n}_{\mathrm{o}} + \varepsilon \boldsymbol{n}_1 \\ \tau(\chi) = \tau_{\mathrm{o}} + \varepsilon\tau_1 \end{array}\right\}. \tag{20}$$

After inserting (15) through (20) into the basic Eqs. (6) through (11) we find first that

$$\left.\begin{array}{l} \operatorname{div} \boldsymbol{u}_1 = 0, \\ \nabla\psi_{\mathrm{o}} = \mu_{\mathrm{w}} \nabla^2 \boldsymbol{u}_1, \\ \boldsymbol{u}_1(\chi_{\mathrm{o}}) \cdot \boldsymbol{n}_{\mathrm{o}} = 0, \\ \tau_{\mathrm{o}} \cdot D[\boldsymbol{u}_1(\chi_{\mathrm{o}}) - \boldsymbol{v}_{\mathrm{o}}(\chi_{\mathrm{o}})] \cdot \boldsymbol{n}_{\mathrm{o}} = 0. \end{array}\right\}. \tag{21}$$

This problem may be solved for $\boldsymbol{u}_1(\chi)$, and $\psi_{\mathrm{o}}(\chi)$ and $\chi_{\mathrm{o}}$ is given. The slow motion in the oil core is driven by the shear rate in the water

$$\tau_{\mathrm{o}} \cdot D[\boldsymbol{v}_{\mathrm{o}}] \cdot \boldsymbol{n}_{\mathrm{o}} = \partial \boldsymbol{v}_{\tau}(\chi_{\mathrm{o}})/\partial y_{\mathrm{n}} \stackrel{\mathrm{def}}{=} \dot{\gamma}(\chi_{\mathrm{o}}), \tag{22}$$

where $\boldsymbol{v}_{\tau}(\chi_{\mathrm{o}})$ is the velocity component tangent to the interface and $y_n$ is normal at $\chi = \chi_{\mathrm{o}}$.

The normal stress balance Eq. (11) now becomes

$$-\phi_{\mathrm{o}}(\chi_{\mathrm{o}}) + \psi_{\mathrm{o}}(\chi_{\mathrm{o}}) - (\rho_{\mathrm{w}} - \rho_{\mathrm{o}})\boldsymbol{g} \cdot \chi_{\mathrm{o}} - 2\mu_{\mathrm{w}} \boldsymbol{n}_{\mathrm{o}} \cdot D[\boldsymbol{u}_1(\chi_{\mathrm{o}})] \cdot \boldsymbol{n}_{\mathrm{o}} = 2H(\chi_{\mathrm{o}})\sigma. \tag{23}$$

We may write

$$\boldsymbol{n}_{\mathrm{o}} \cdot D[\boldsymbol{u}_1(\chi_{\mathrm{o}})] \cdot \boldsymbol{n}_{\mathrm{o}} = \partial \boldsymbol{u}_{1\mathrm{n}}/\partial y_{\mathrm{n}},$$

where $\boldsymbol{u}_{1n}$ is the normal component of $\boldsymbol{u}_1$ at the interface point $\chi = \chi_o$. In deriving Eq. (23) we used an easily proved result which says that

$$\boldsymbol{n}_o \cdot D[\boldsymbol{v}(\chi_o)] \cdot \boldsymbol{n}_o = 0,$$

when $\boldsymbol{v}_o(\chi_o)$ is the fluid velocity at the boundary of a rigid body. Eq. (23) selects $\chi_o$ which until now was arbitrary.

The perturbation equations at higher order were presented by Joseph and Bai (1999).

## 5. Core-annular flow

Here we shall revisit the problem of waves on core-annular flow considered by Bai et al. (1996). They treated a steady flow in which the holdup ratio $c_o/c_w$ of average velocities $c_o = Q_o/\pi R_1^2 \approx (Q_o + \varepsilon Q_1)/\pi R_1^2$ and $c_w = Q_w/(R_2^2 - R_1^2)$ is prescribed. Here $Q_o$ and $Q_w$ are the volume flux of oil and water, $R_2$ is the outer radius of the pipe and $R_1$ is the mean radius of the core. In the approximation carried out by them, the core is rigid. The analysis of the steady flow of water is carried out in a coordinate system in which the core is stationary; secondary motions in the core were not treated. The shape of the interface was computed using the normal stress condition under the assumption that the pressure in the core is uniform apart from a constant pressure gradient $\beta$ along the pipe axis $z$ (see Fig. 1).

The problem of core-annular flow may be treated in the framework of perturbation theory described in Section 3 and 4 with $\lambda \cdot \chi$ in (5) equation to $-\beta \boldsymbol{e}_z \cdot \boldsymbol{z}$ where $\beta$ is a constant gradient. The governing equations at zero-th order are essentially Eq. (14).

$$\left.\begin{array}{l} \rho_w \boldsymbol{v} \cdot \nabla \boldsymbol{v} = \beta \boldsymbol{e}_z - \nabla p_w + \mu_w \nabla^2 \boldsymbol{v}, \\ \boldsymbol{v} = 0 \quad \text{on } r = f(z), \\ \boldsymbol{v} = -c\boldsymbol{e}_z \quad \text{on } r = R_2 \end{array}\right\}, \tag{24}$$

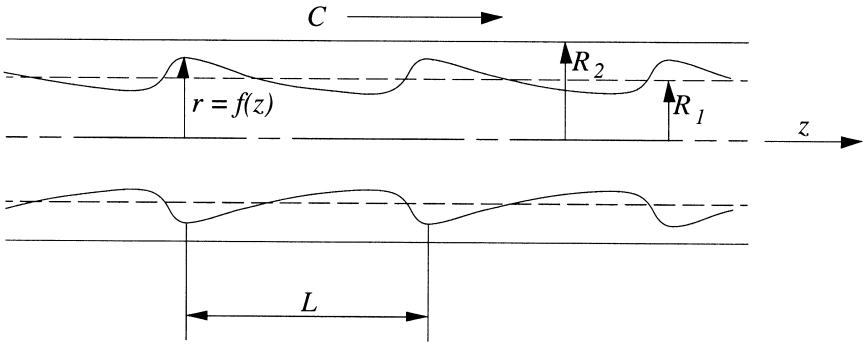


Fig. 1. The wave core-annular flow is periodic $L$. The mean radius is $R_1$ where $R_1^2 = 1/L \int_0^L f^2(z)\mathrm{d}z$. The core moves backward with velocity $c$ and the wall is stationary; here the core has been put to rest and the wall moves forward. Let $\Omega_w$ be the domain occupied by water $0 \le z \le L$, $f(z) \le r \le R_2$ and $\Omega_o$ is the domain occupied by oil $0 \le z \le L$, $0 \le r < f(z)$.

where $r = f(z)$ gives the shape of the interface and $f(z)$ was determined by Bai et al. (1996) using the normal stress condition

$$\frac{\sigma}{f(1+f'^2)^{1/2}} - \frac{\sigma f''}{(1+f'^2)^{3/2}} = C - p_w. \tag{25}$$

The ratio of the average oil to water velocity $h = c/c_w$, is given by

$$h = \frac{Q_o/Q_w}{R_1^2/(R_2^2 - R_1^2)} = \frac{\pi c R_1^2}{\pi c[f^2 - R_1^2] + 2\pi \int_f^{R_2} r v \mathrm{d}r} \frac{R_2^2 - R_1^2}{R_1^2}. \tag{26}$$

Though $f$ depends on $z$, $h$ is a constant, independent of $z$; $h = 2$ for perfect core flow without waves and $h = 1$ when the water is trapped between wave crests touching the pipe wall. For wavy flow $1 < h < 2$; $h = 1.4$ occurs frequently in experiments; the selection mechanism is related to stability and is not understood. Bai et al. (1996) prescribed $h = 1.4$, ensuring waves.

Going further now than Bai et al. (1996) we consider now the problem (21) for the flow $\boldsymbol{u} = \boldsymbol{u}_1$ in the oil core

$$\left.\begin{aligned} &\operatorname{div} \boldsymbol{u} = 0 \\ &-\beta \boldsymbol{e}_z + \nabla p_o = \mu_w \nabla^2 \boldsymbol{u} \end{aligned}\right\}, \tag{27}$$

where on $r = 0$, we have

$$u_r = 0, \quad \frac{\partial u_z}{\partial r} = 0,$$

and on $r = f(z)$, we have

$$\boldsymbol{u}(r, z) \cdot \boldsymbol{n} = 0 \tag{28}$$

and

$$\tau \cdot D[\boldsymbol{u}] \cdot \boldsymbol{n} = \dot{\gamma}(r, z), \tag{29}$$

where the shear rate

$$\dot{\gamma}(f(z), z) = \tau \cdot D[\boldsymbol{v}_o] \cdot \boldsymbol{n} \tag{30}$$

is evaluated on the solution $\boldsymbol{v}_o$ of Eqs. (24–26). The constant $\beta$ and $\dot{\gamma}(r, z)$ are prescribed.

After computing $\boldsymbol{v}_o$ and $p_w$ from the problem (24) and $\boldsymbol{u}$ and $p_o$ from the problem (27–30), we may complete the perturbation cycle by forming the normal stress balance corresponding to Eq. (23). This balance replaces Eq. (25) with

$$\frac{\mathrm{d}^2 f}{\mathrm{d}z^2} - \frac{1 + (\mathrm{d}f/\mathrm{d}z)^2}{f} + \frac{1}{\sigma}\left(1 + \left(\frac{\mathrm{d}f}{\mathrm{d}z}\right)^2\right)^{3/2} (C_p + p_o(z) - p_w(z) + 2\mu_w \boldsymbol{n} \cdot D[u] \cdot \boldsymbol{n}) = 0. \tag{31}$$

Equation (31) cannot be satisfied for arbitrarily selected functions $r = f(z)$ and wavelength $L$.

These parameters are iterated at each perturbation cycle until Eq. (31) balances and holdup ratio Eq. (26) is met, giving rise to converged values of $f(z)$ and $L$.

## 6. Numerical method and procedure

The numerical method follows along lines introduced by Bai et al. (1996). Axisymmetric core-annular flow is governed by Eq. (24) at zero-th order and by Eq. (27) at first order subject to the normal stress condition specified by Eq. (28), the shear stress condition specified by Eq. (29) and Eq. (30) and the normal stress balance is given by Eq. (31). For each prescription of three control parameters ($c$, $R_1$, $h$), fluid properties $\rho$, $\mu$, $\sigma$ and the pipe radius $R_2$, the computational solution is carried out first for the flow field in the water and then in the perturbed core; the pressure gradient driving the flow, the pressure distributions and the wave shape are computed. The computation involves iteration between the flow fields at zero-th order in the water and at first order in the core, and the calculation of the free surface.

Equation (24) is a Dirichlet problem for the Navier–Stokes equations which gives the flow of water at zero-th order. The control volume method of Patankar (1980) is used for the numerical solution. The force due to the pressure difference in one wavelength is balanced by the force due to the shear stress on the pipe wall:

$$\pi R_2^2 L\beta = 2\pi R_2 \int_0^L \left( \mu_2 \frac{\mathrm{d}u}{\mathrm{d}r}\bigg|_{r=R_2} \right) \mathrm{d}z. \tag{32}$$

Further details are given by Bai et al. (1996).

The perturbed flow field in the core is governed by Eq. (27). These equations define a Dirichlet problem for Stokes equations. The core is defined by the same prescribed wave shape $f$ and the flow of oil in the core is driven by a prescribed shear strain (29) and pressure gradient $\beta$ determined by the flow of water at zero-th order. The zero-th and first order problems are decoupled.

The computation of the wave shape involves an iterative solution of the normal stress balance Eq. (31) using values for the pressure jump and the jump in the viscous part of the normal stress from solutions at zero-th and first order. In general, the normal stress balance will not be satisfied, so that an iterative procedure in which the shape function $f(z)$ is changed must be implemented.

The discretized form of Eq. (31) is generated as follows. The unknown shape $f(z)$ is represented by discrete values of $f$ at the same $z$ locations used in the calculation of the flow of water. The equations for these values of $f(z)$ are constructed by integrating (31) over the main control volumes in the $z$-direction. The last term in the equation is treated explicitly as a source term and is assumed to be constant over the control volume. The resulting equation has the following form.

$$a_i f_i = b_i f_{i+1} + c_i f_{i-1} + S\Delta z_i, \tag{33}$$

where

$$b_i = \frac{1}{z_{i+1} - z_i}, \quad c_i = \frac{1}{z_i - z_{i-1}}, \quad a_i = b_i + c_i + \frac{1 + (\mathrm{d}f_i^*/\mathrm{d}z)^2}{f_i^{*2}}\Delta z_i,$$
$$S_i = \frac{1}{\sigma}\left(1 + \left(\frac{\mathrm{d}f_i^*}{\mathrm{d}z}\right)^2\right)^{3/2}(C_p + p_{\mathrm{oi}}^{**} - p_{\mathrm{wi}}^{**} + 2\mu_{\mathrm{w}}(\boldsymbol{n} \cdot D[\boldsymbol{u}] \cdot \boldsymbol{n})_i), \tag{34}$$

and

$$\Delta z_i = (z_{i+1} - z_{i-1})/2.$$

As in the calculation of the flow, the periodicity of $f_i$ is accounted by recognizing that in the equation for $f_N$, $f_{N+1}$ is replaced by $f_1$ while in the equation for $f_1$, the $f_{1-1}$ is replaced by $f_N$. The single $^*$ in Eq. (33) marks the variables that are updated within the inner iteration for determining the free surface shape while the decpuple $^{**}$ on $p_i$ denote that these values are kept constant during the free surface calculation and are updated only in the outer iteration.

The unknown pressure jump $C_p$ and the wavelength $L$ provide the two degrees of freedom necessary to determine the free surface shape consistent with specified values of the average plug radius $R_1$ and holdup ratio $h$. After each iteration, during calculation of the $f_i$, the value of $C_p$ is increased or decreased according to whether the available $f_i$ values imply a value of $R_1$ larger or smaller than that desired. Similarly, the wavelength $L$ is increased or decreased if the current value of the holdup ratio $h$ is larger or smaller than its prescribed value. The amount of adjustment in the values of $C_p$ and $L$ is determined using the secant method. It uses the predictions from the last two iterations to determine the sensitivity of $R_1$ and $h$ to changes in $C_p$ and $L$. The sensitivity coefficients are then used for inferring the changes in $C_p$ and $L$ to be made in the next iteration. At convergence, this procedure provides a free surface shape and location having the desired $R_1$ and $h$ for the surface pressure variation determined from the flow field calculation.

The overall solution method involves iteration between the flow of water, oil core and the determination of the free surface. The iterations are decoupled but the overall solution is coupled and related. The steps in the iteration are:

1. Prescribe the values of wave speed $c$, average core radius $R_1$, and the holdup ratio $h$.
2. Assume a free surface shape. Calculate the velocity and pressure fields in the water for the specified wave speed $c$. During each iteration of the flow, the pressure gradient $\beta$ is adjusted to satisfy the force balance on the wall.
3. Use a same free surface shape as in step 2, calculate the velocity and pressure field in the oil using results from the water solution in step 2.
4. The shape of the free surface is determined by satisfying the normal stress balance from the pressure and velocity fields determined in steps 2 and 3. The wavelength and the pressure constant are adjusted in each iteration so that at convergence the free surface shape is determined for the prescribed average core radius $R_1$ and holdup ratio $h$.
5. The new free surface is now used in determining the flow field in step 2 and step 3. Thus, steps 2, 3 and 4 are repeated till convergence to obtain a self-consistent flow of water, oil in which the surface balances are satisfied for the prescribed values of the parameter triplet ($c$, $R_1$, $h$).

The overall solution method correctly predicted the perfect core flow and our solutions always converged to the same wavy core flow, independent of the guess of initial surface shape, for a given set of parameters. These results and the good agreements with experiments indicate that the numerical solutions of the perturbation equations lead to valid representations of steady wavy core flow.

## 7. Dimensionless equations

Analysis of this simulation is most useful when carried out in terms of dimensionless variables in Eqs. (14) and (21) with

$$\bar{\boldsymbol{v}}_{\mathrm{o}} = \frac{\boldsymbol{v}_{\mathrm{o}}}{U}, \quad \bar{\boldsymbol{u}}_1 = \frac{\boldsymbol{u}_1}{U}, \quad \bar{\phi}_{\mathrm{o}} = \frac{\phi_{\mathrm{o}}}{\rho_2 U^2}, \quad \bar{\psi}_{\mathrm{o}} = \frac{\psi_{\mathrm{o}}}{\rho_2 U^2}, \quad \bar{r},\ \bar{z},\ \bar{f},\ \bar{L} = \frac{r}{R_2},\ \frac{z}{R_2},\ \frac{f}{R_2},\ \frac{L}{R_2},$$

$$R_1^2 = \frac{1}{L}\int_0^L f^2 \mathrm{d}z = \frac{R_2^2}{L}\int_0^{\bar{L}} \bar{f}^2 \mathrm{d}\bar{z}, \quad \eta^2 = \frac{R_1^2}{R_2^2} = \frac{1}{L}\int_0^{\bar{L}} \bar{f}^2 \mathrm{d}\bar{z}, \quad \mathscr{R} = \frac{\rho_{\mathrm{w}} R_2 U}{\mu_{\mathrm{w}}} = \frac{\rho_{\mathrm{w}}(R_2 - R_1)c}{\mu_{\mathrm{w}}}.$$

The relationship between $U$ and $c$ is

$$c = \frac{UR_2}{(R_2 - R_1)} = \frac{U}{1-\eta}. \tag{35}$$

We may define a dimensionless wall speed

$$\bar{c} = \frac{c}{U} = \frac{1}{1-\eta}. \tag{36}$$

Therefore, at the boundary

$$\bar{\boldsymbol{v}}_{\mathrm{o}}(\bar{v}_{r\mathrm{o}}, \bar{v}_{z\mathrm{o}}) = (0,\ \bar{c}), \quad \text{at } \bar{r} = 1.$$

$$\bar{\boldsymbol{u}} = (\bar{u}_r,\ \bar{u}_z),$$

$$\bar{u}_r = 0, \quad \frac{\partial \bar{u}_z}{\partial \bar{r}} = 0 \quad \text{at } \bar{r} = 0.$$

At the interface, the normal stress balance with pressure jump becomes

$$\frac{S}{\bar{f}\sqrt{1 + (\mathrm{d}\bar{f}/\mathrm{d}\bar{z})^2}} - \frac{S(\mathrm{d}^2\bar{f}/\mathrm{d}\bar{z}^2)}{(1 + (\mathrm{d}\bar{f}/\mathrm{d}\bar{z}))^{3/2}} - 2\frac{\boldsymbol{n}\cdot D[\bar{\boldsymbol{u}}]\cdot \boldsymbol{n}}{\mathscr{R}} = [[\bar{P}]], \tag{37}$$

where

$$S = \frac{\sigma}{\rho_{\mathrm{w}} U^2 R_2} = \frac{J}{\mathscr{R}},$$

and

$$J = \frac{\rho_w R_2 \sigma}{\mu_w^2}.$$

The dimensionless oil flow rate

$$\bar{Q}_o = \frac{Q_o}{UR_2^2} = \frac{\pi\bar{c}}{\bar{L}}\int_0^{\bar{L}} \bar{f}^2 d\bar{z} = \pi\bar{c}\eta^2 = \frac{\pi\eta^2}{1-\eta^2}, \tag{38}$$

is determined if $\eta$ is given.

The dimensionless water flow rate may be expressed by holdup ratio $h$ and $\eta$ as

$$\bar{Q}_w = \frac{Q_w}{R_2^2 U} = \frac{1}{R_2^2 U}\int_{R_1}^{R_2} 2\pi r c_w dr = \frac{2\pi}{h}\int_\eta^1 \bar{c}\bar{r}d\bar{r} = \frac{\pi(1-\eta^2)}{(1-\eta)h} = \frac{\pi(1+\eta)}{h}. \tag{39}$$

Four parameters are required for a complete description of our problem:

$\mathscr{R}$, $\eta$, $J$ and $h$.

All possible problems of scale up can be solved in this set of parameters.

In our computation we choose $J = 13 \times 10^4$ corresponding to the actual physical parameters in wavy core flow in water ($\mu_2 = 0.01$ P $\rho = 1.0\text{g/cm}^3$, $\sigma = 26\text{dyn/cm}$) flowing in pipe of radius $R_2 = 0.5$. For the plots in Section 8 we use the dimensionless pressure

$$\bar{p} = \frac{p}{\rho_2 U^2} = \frac{p}{\mathscr{R}^2}\frac{\rho_2 R_2^2}{\mu^2} = \frac{p^*}{\mathscr{R}^2}, \tag{40}$$

$$p^* = \frac{p}{\mu_2^2}\rho R_2^2 \tag{41}$$

and pressure gradient

$$\beta^* = \frac{\beta}{\mu_2^2}\rho R_2^2 \tag{42}$$

The dimensionless viscous part of the normal stress is

$$N^* = 2\boldsymbol{n}\cdot\overline{D[\boldsymbol{u}]}\cdot\boldsymbol{n}\mathscr{R}. \tag{43}$$

We prefer to use a Reynolds number

$$\mathbb{R} = \frac{\rho(R_2 - R_1)c}{\mu_2} \tag{44}$$

based on the gap size instead of $R$ in the presentation of the results given below.

## 8. Numerical results

Here we give results for the perturbation theory and compare them with the rigid deformable core approximation computed by Bai et al. (1996).

Figure 2 gives the pressure distributions and the viscous contribution to the normal stress along the wavy interface; the pressure in the core and the viscous contribution to the normal stress are relatively small.

Figure 3 compares wave shapes given by the perturbation theory and the rigid approximation when $[\eta,\ h,\ \mathbb{R},\ J] = [0.8,\ 1.4,\ 600,\ 13 \times 10^4]$. The wave shapes are slightly different because of the small additional contribution to the normal stress due to the secondary motion in the core. The perturbed wavelength is also slightly longer.

Figure 4 shows that the wavelength decreases with $\mathbb{R}$ and the pressure gradient increases linearly with $\mathbb{R}$ for fixed values of $[\eta,\ h,\ J] = [0.8,\ 1.4,\ 13 \times 10^4]$; the values of the pressure gradient are identical, but the wave length given by perturbation theory is greater than the wavelength given by the rigid core approximation.

Figure 5 shows how the wavelength and pressure gradient vary with holdup ratio $h$ when $[\eta,\ \mathbb{R},\ J] = [0.8,\ 1.4,\ 13 \times 10^4]$; they both decrease with $h$. The difference between the wavelengths from perturbation theory and rigid core approximation is bigger when the holdup ratio $h$ is smaller. The pressure gradients from both approaches are essentially the same.

Figure 6 shows how the wavelength and pressure gradient vary with the core diameter $\eta$ when $[h,\ \mathbb{R},\ J] = [1.4,\ 600,\ 13 \times 10^4]$. The pressure gradients increase with $\eta$ and the wavelengths decrease linearly with $\eta$:

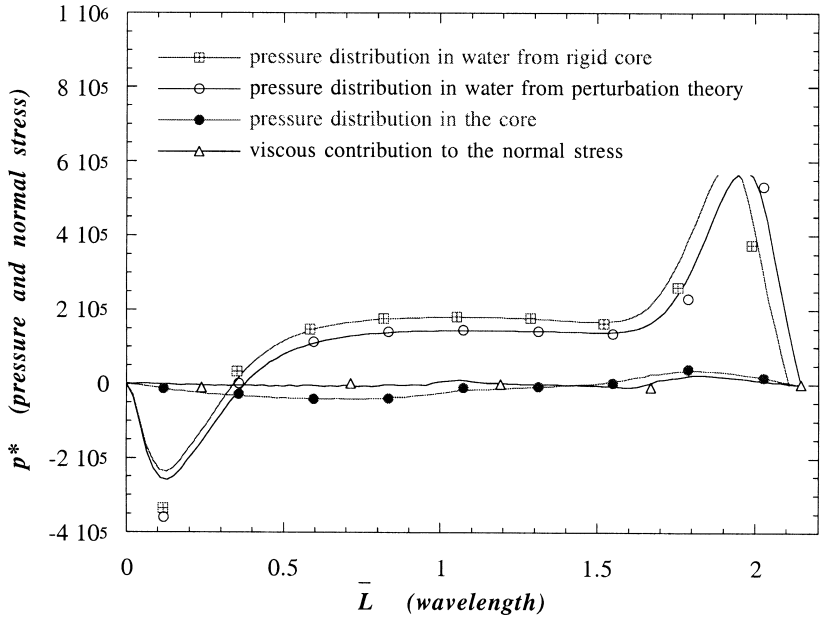


Fig. 2. The pressure distributions and viscous contribution normal stress along the wave interface when $[\eta, h, \mathbb{R}, J] = [0.8, 1.4, 600, 13 \times 10^4]$.

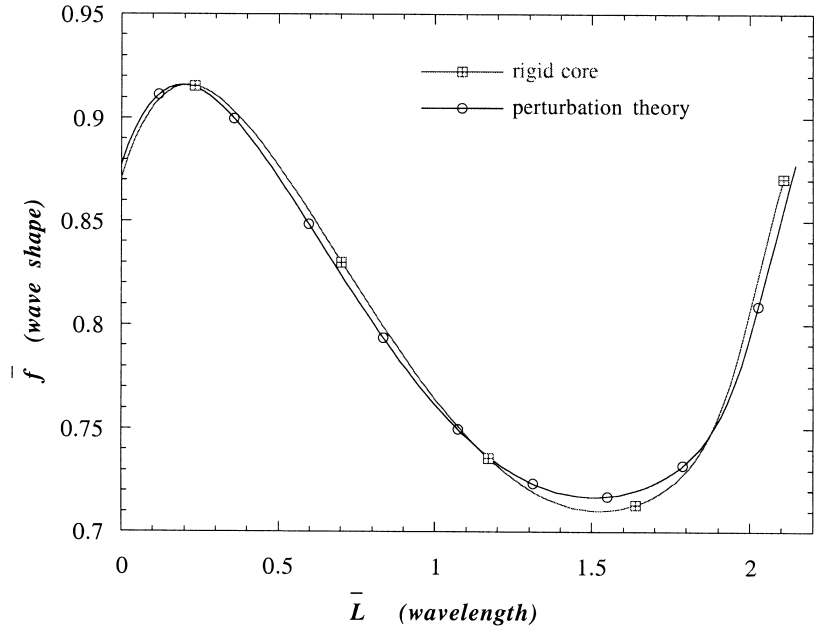


Fig. 3. Wave shapes from perturbation theory and rigid approximation when $[\eta, h, \mathbb{R}, J] = [0.8, 1.4, 600, 13 \times 10^4]$.

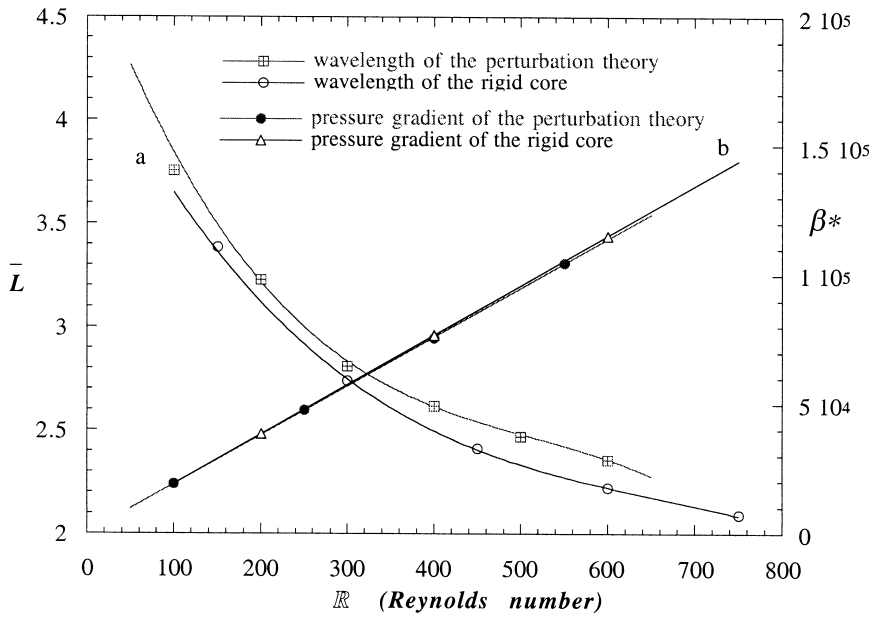


Fig. 4. (a) Dimensionless wavelength $\bar{L}$ vs. Reynolds number $\mathbb{R}$ for the perturbation theory and for the rigid core approximation solution when $[\eta, h, J] = [0.8, 1.4, 13 \times 10^4]$; (b) Pressure gradient $\beta^*$ vs. $\mathbb{R}$ under the same conditions.

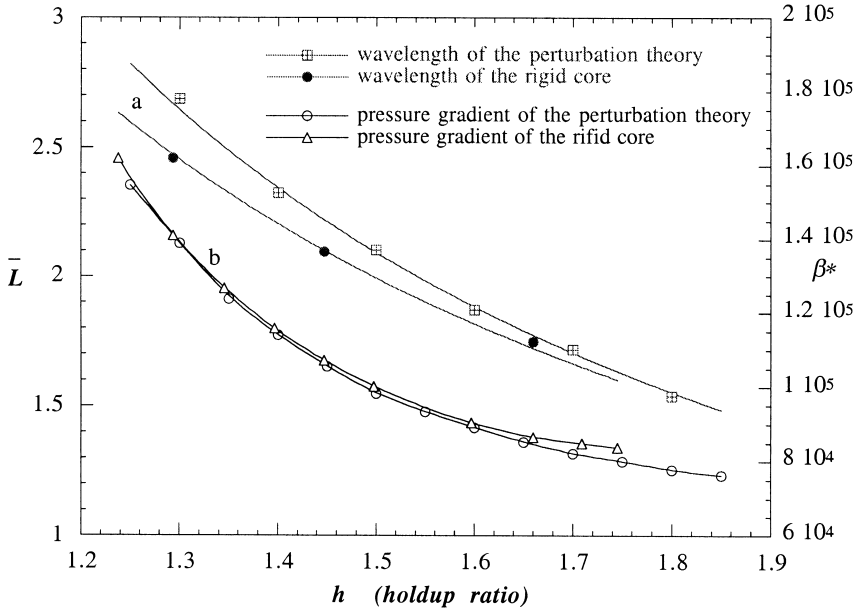


Fig. 5. (a) Dimensionless wavelength $\bar{L}$ vs. holdup ratio $h$ when $[\eta, \mathbb{R}, J] = [0.8, 600, 13 \times 10^4]$; (b) Pressure gradient $\beta^*$ vs. $h$ under the same conditions.

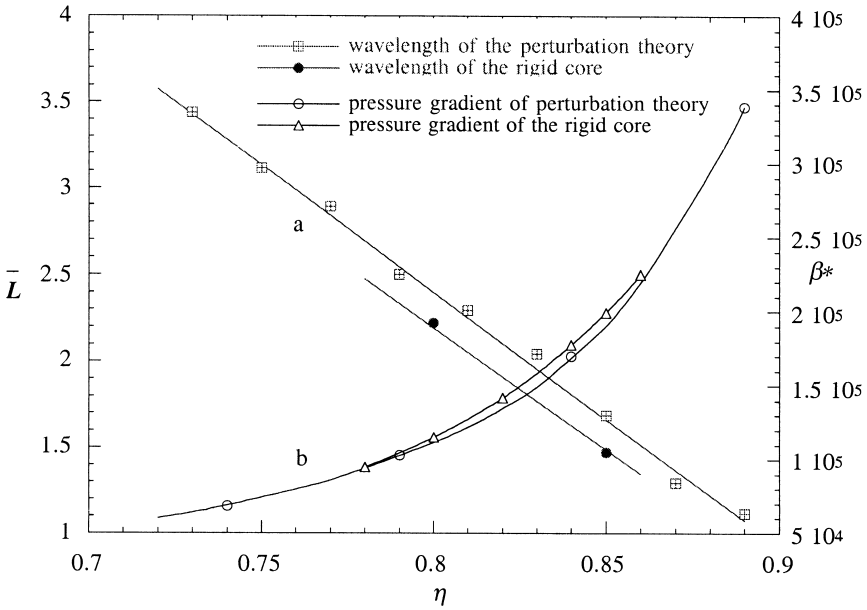


Fig. 6. (a) Dimensionless wavelength $\bar{L}$ vs. core diamer $\eta$ when $[\mathbb{R}, h, J] = [600, 1.4, 13 \times 10^4]$; (b) Pressure gradient $\beta^*$ vs. $\eta$ under the same conditions.

$\bar{L}_p(\eta) = a_1 - b\eta$ from perturbation,

and

$\bar{L}_R(\eta) = a_2 - b\eta$ from rigid core approximation.

Figure 7 shows that the effect of surface tension is to smooth the waves and increase the wavelength. The wavelength computed by perturbation theory is slightly greater than the wavelength computed with the approximation theory.

Figure 8 gives streamlines for the rigid core approximation and the perturbation when $[\eta, h, \mathbb{R}, J] = [0.8, 1.4, 600, 13 \times 10^4]$. Figure 8(a) shows the streamlines in the water when the core is rigid while Fig. 8(b) shows the streamlines for the perturbed theory. The streamlines in the water in the two cases are nearly the same. The streamlines in the core are monotone without eddies. The normal stress at first order is the seem of a first order contribution to the pressure and a contribution to the viscous part of the normal stress. The normal stress at zero-th order is only from the pressure and it is much larger than the normal stress at first order. The shape of the interface is mainly determined by the pressure at zero-th order. The secondary motion in wave trough is caused by the friction between the core and wall. The high pressure not only sharpens the wave front, but also produces a levitation force which pushes the core away from the wall.

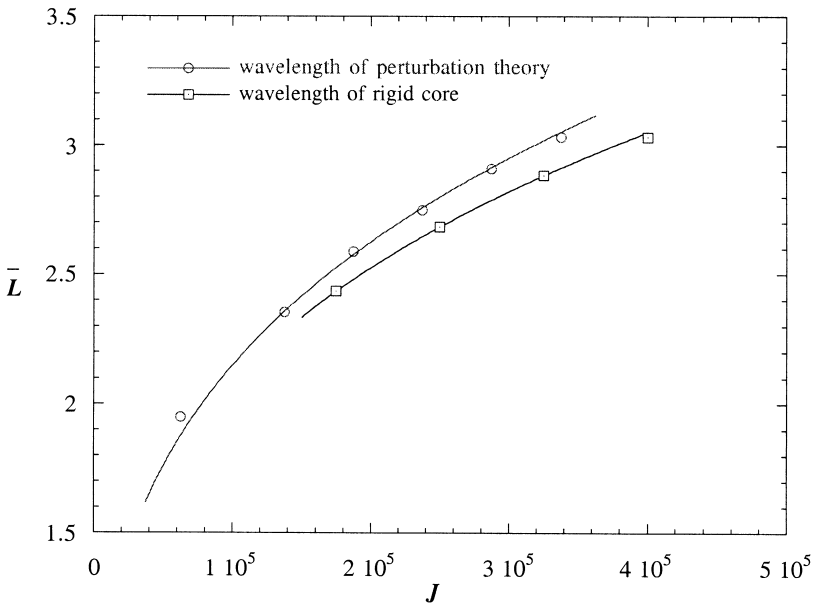


Fig. 7. Dimensionless wavelength $\bar{L}$ vs. interfacial tension $J$ when $[\eta, h, \mathbb{R}] = [0.8, 1.4, 600]$.

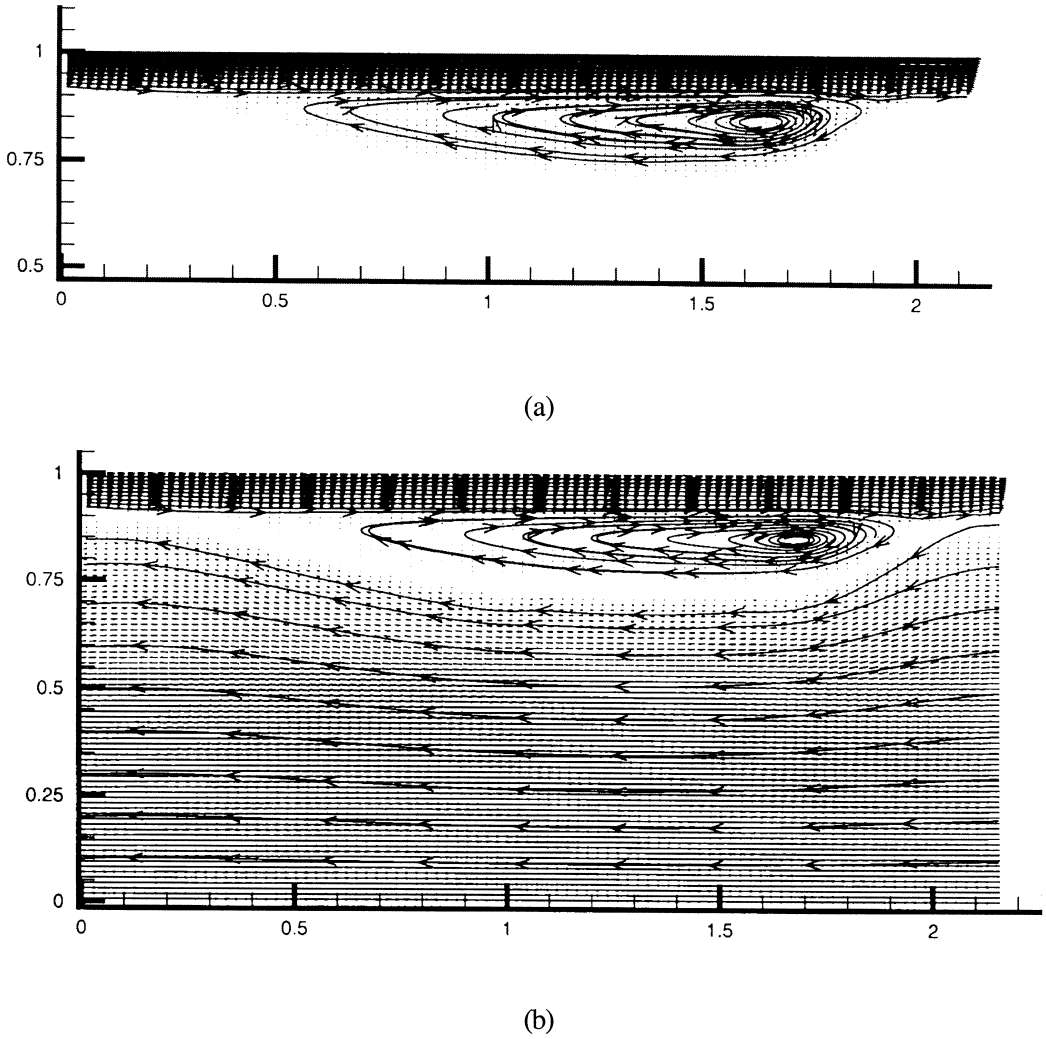


Fig. 8. Streamlines and secondary motion for (a) rigid core and (b) pertubation theory when $[\eta, h, \mathbb{R}, J] = [0.8, 1.4, 600, 13 \times 10^4]$.

## 9. Comparison with experiments

Bai et al. (1992) did experiments and calculated stability results for vertical axisymmetric core flow in the case when the buoyant force and pressure force on the oil are both against gravity (up flow). They observed 'bamboo' waves for their oil $\rho_o = 0.905$ g/cm$^3$ and $\mu_o = 6.01$ P in water with $\rho_w = 0.995$ g/cm$^3$ and $\mu_w = 0.01$ P. Bai et al. (1996) simulated the same flow, with the same parameters except that the core was assumed to be infinitely viscous. Here we shall show that the computed wave shapes and other features of the flow are in better agreement with experiments when the motion in the core is not suppressed. The equations for

Table 1
Comparison of computed and measured values of the wave speed $c$ and wave length $L$. The holdup $h = 1.39$ in all computations and in the experiments

| No. | Input flowrate | | I Perturbation theory | | Experiments | | II Rigid core | | III Stability theory | |
|---|---|---|---|---|---|---|---|---|---|---|
| | $Q_o$ | $Q_w$ | $L$ (cm) | $c$ (cm/s) | $L$ (cm) | $c$ (cm/s) | $L$ (cm) | $c$ (cm/s) | $L$ (cm) | $c$ (m/s) |
| (1) | 25.38 | 13.17 | 1.16 | 55.59 | 1.21 | 57.7 | 1.32 | 55.59 | 0.79 | 52.02 |
| (2) | 18.19 | 13.17 | 1.31 | 46.45 | 1.31 | 43.28 | 1.66 | 46.45 | 0.96 | 42.54 |
| (3) | 11.01 | 13.17 | 1.64 | 37.30 | 1.41 | 35.65 | 1.70 | 37.30 | 1.22 | 33.51 |
| (4) | 7.42 | 13.17 | 2.19 | 32.73 | 1.22 | 27.81 | 1.33 | 32.73 | 1.33 | 29.42 |
| (5) | 7.42 | 6.46 | 1.38 | 20.88 | 1.374 | 19.16 | 1.77 | 20.88 | 1.25 | 17.94 |
| (6) | 11.01 | 6.46 | 1.36 | 25.45 | 1.79 | 22.90 | 1.66 | 25.45 | 1.16 | 22.17 |
| (7) | 14.60 | 6.46 | 1.18 | 30.02 | 1.34 | 28.22 | 1.39 | 30.02 | 1.02 | 26.68 |
| (8) | 18.19 | 6.46 | 1.04 | 34.59 | 1.17 | 31.06 | 1.15 | 34.59 | 0.87 | 31.33 |
| (9) | 21.78 | 6.46 | 0.91 | 39.17 | 0.90 | 36.25 | 0.96 | 39.17 | 0.79 | 35.71 |

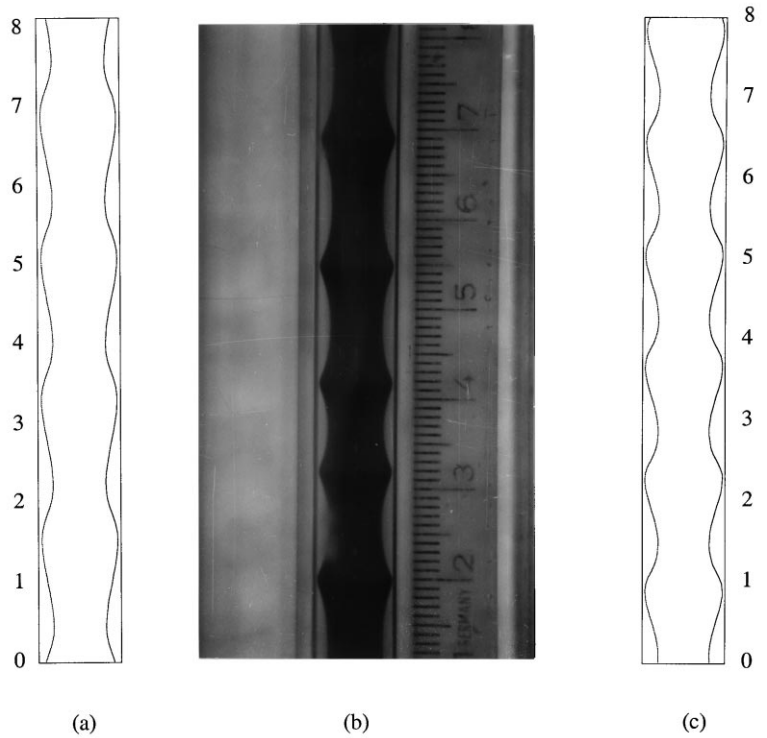


Fig. 9. Comparison of theory and experiment when $[Q_w, Q_o] = [200, 429]\, cm^3\, min^{-1}$: (a) Rigid core computation and (b) experiment from Bai et al. (1996), (c) perturbation theory of this paper.

vertical flow are given in Section 2 with Eq. (5) replaced by

$$\left.\begin{aligned}\psi &= p_o + \lambda\cdot\chi + \rho_o \boldsymbol{g}\cdot\chi - \rho_c \boldsymbol{g}\cdot\chi \\ \phi &= p_w + \lambda\cdot\chi + \rho_w \boldsymbol{g}\cdot\chi - \rho_c \boldsymbol{g}\cdot\chi\end{aligned}\right\} \tag{45}$$

where $\rho_c$, is the composite density of the mixture

$$\rho_c = \rho_o\eta^2 + \rho_w(1-\eta^2). \tag{46}$$

We compared wavelengths, wave speeds and wave shapes from our computation with experiments and the linear theory of stability given by Bai et al. (1992). In our comparison, the flow parameters are based on the experimental information, such as flow rates of oil and water, oil volume ratio and holdup ratio. Bai et al. (1992) found the holdup ratio is very nearly a constant 1.39 in experiments for a wide range flow rates.

The comparison of computed and measured values of the wave speed $c$ and wave length $L$ of bamboo waves is given in Table 1. Column I gives the values of $c$ and $L$ from the perturbation theory presented in this paper. Column II presents results for the rigid deformable core computed by Bai et al. (1996). Column III give results from the linear theory of stability of perfect core flow given by Bai et al. (1992). These calculations were done for prescribed values $Q_o$ of the oil flow and measured values $h = 1.39$ of the holdup ratio; the values $c$ and $L$

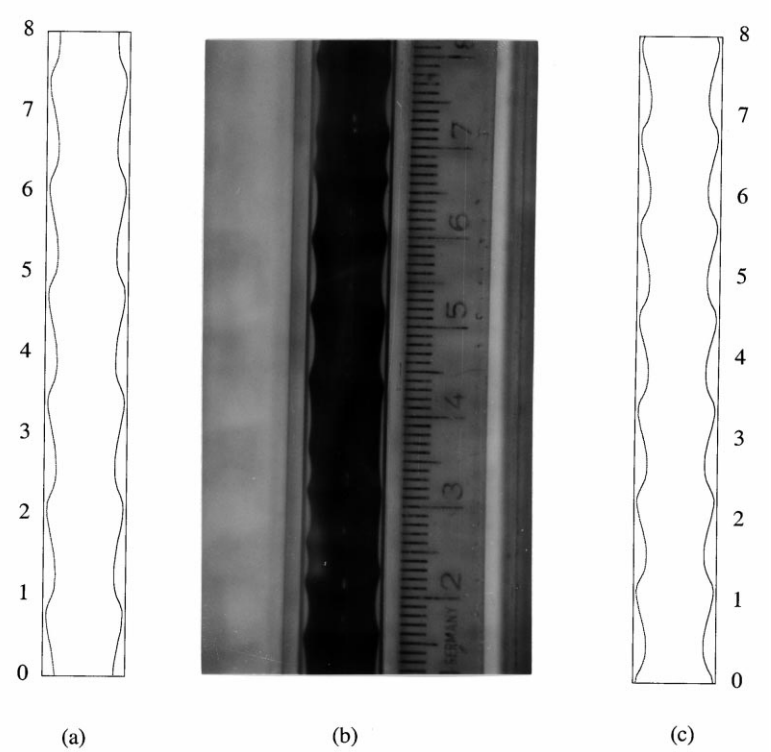


Fig. 10. Comparison of theory and experiment when $[Q_w, Q_o] = [200, 825]\, cm^3\, min^{-1}$: (a) Rigid core computation and (b) experiment from Bai et al. (1996), (c) perturbation theory.

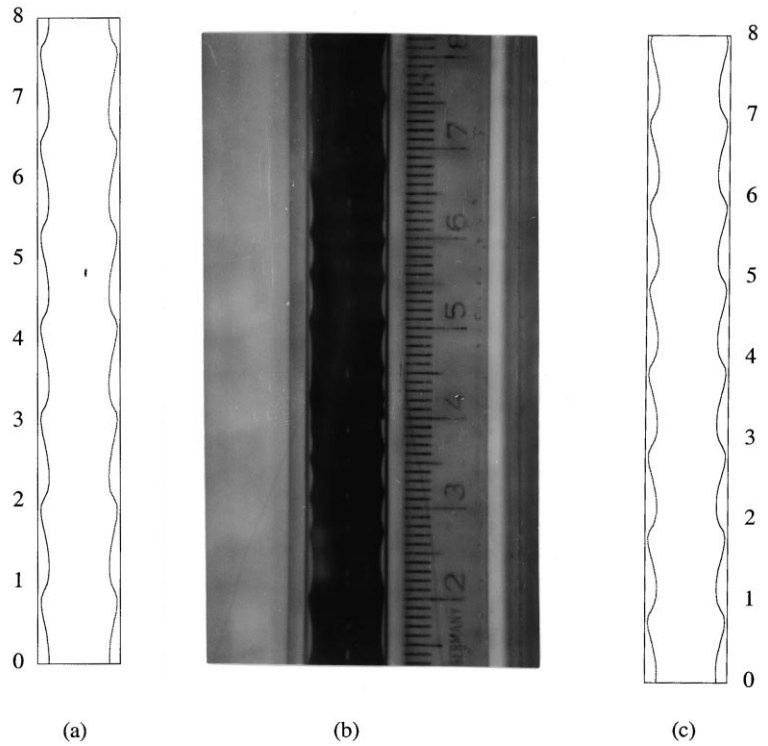


Fig. 11. Comparison of theory and experiment when $[Q_w, Q_o] = [200, 1216]\, cm^3\, min^{-1}$: (a) Rigid core computation and (b) experiment from Bai et al. (1996), (c) perturbation theory.

belong to the wave with the maximum growth rate. The values of $\eta$ and $\mathbb{R}$ in all computations correspond to the given values of $Q_o$ and $Q_w$ for $h = 1.39$ and $\sigma = 22.5$ (dyn/cm) ($J = 11.2 \times 10^4$). The values ($\eta$, $\mathbb{R}$) are 1 (0.76, 661), 2 (0.7, 683), 3 (0.61, 722), 4 (0.54, 758), 5 (0.67, 342), 6 (0.74, 328), 7 (0.79, 320), 8 (0.82, 314) and 9 (0.84, 310).

It is apparent from comparison of the experimental values with computed ones that our perturbation theory gives rise to the most accurate results, as expected. The results from the liner theory of stability of perfect core flow are less accurate, but actually rather good considering that the observed flows can hardly be described as a small perturbation of perfect core flow.

Computed and observed shapes of bamboo waves on motor oil in water in a vertical pipeline are compared in Fig. 9–11 ($\rho_o = 0.905$ g/cm$^3$, $\mu_o = 6.01$ P) and water ($\rho_w = 0.995$ g/cm$^3$, $\mu_w = 0.01$ P). The pressure gradient and buoyant force on the oil are both against gravity; the core is 'stretched' by buoyancy. The water flow rate is fixed at 200 cm$^3$/min while the oil flow rate is 429, 825 and 1216 cm$^3$/min.

## 10. Conclusion

We have presented a perturbation theory for the steady flow and interface shapes of a highly

viscous dispersed phase. The theory is based on a regular expansion in powers of the viscosity ratio and it generates a series of uncoupled Dirichlet problems in the water and, Stokes flow in the core, in which the shape of the interface is iterated with the normal stress balance. The theory was applied to the problem of core-annular flow and compared with an earlier approximate theory in which the relative motion in the core and the pressure variations there were neglected. The approximate theory gives rise to small errors which are put right by the present theory; satisfactory agreements of the lowest order exact theory with experiments are exhibited and even better agreements might be expected the higher order theory.

The computations given in the paper all prescribe the value $h = 1.39$ of the holdup ratio which was observed in the experiments of Bai et al. (1992) for bamboo waves in up flow in a wide variety of circumstances. In fact $h$ is a functional of the solution of the initial value problem which was not solved here. Presumably, the value of $h$ ($\approx 1.39$) which occurs in up flow experiments would arise from a stability analysis of different steady solutions corresponding to different values of $h$. The mechanism of selection of a holdup value for given values of the volume flow rate of oil and water needs further elucidation.

## Acknowledgements

This work was supported by the Department of Energy, Office of Basic Energy Science and Minnesota Supercomputer Institute.

## References

Arney, M.S., Bai, R., Guevara, E., Joseph, D.D., Liu, K., 1993. Friction factor and holdup studies for lubricated pipelining. Int. J. Mult. Flow 19, 1061–1076.

Bai, R., Chen, K., Joseph, D.D., 1992. Lubricated pipelining: stability of core-annular flow. Part 5: experiments and comparison with theory. J. Fluid Mech. 240, 97–142.

Bai, R., Kelkar, K., Joseph, D.D., 1996. Direct simulation of interfacial waves in a high viscosity ratio and axisymmetric core-annular flow. J. Fluid Mech. 327, 1–34.

Charles, M.E., 1963. The pipeline flow of capsules. 2. Theoretical analysis of the concentric flow of cylindrical forms. Can. J. Chem. Eng. 46.

Charles, M.E., Govier, G.W., Hodgson, G.W., 1961. The horizontal pipeline flow of equal density of oil–water mixtures. Can. J. Chem. Eng. 39, 17–36.

Chen, K., Bai, R., Joseph, D.D., 1990. Lubricated pipelining. 3. Stability of core-annular flow in vertical pipes. J. Fluid Mech. 214, 251–286.

Clark, A.F., Shapiro, A., 1949. US Patent No. 2,533,878.

Clifton, E.G., Handley, L.R., 1958. US Patent No. 2,821,205.

Feng, J., Huang, P.Y., Joseph, D.D., 1995. Dynamic simulation of the motion of capsules in pipelines. J. Fluid Mech. 286, 201–227.

Glass, W., 1961. Water addition aids pumping viscous oils. Chem. Eng. Prog. 57, 116.

Ho, W.S., Li, N.N., 1994. Core-annular flow of liquid membrane emulsion. AIChE J. 40 (12), 1961–1968.

Isaacs, J.D., Speed, J.B., 1904. US Patent No. 759,374.

Joseph, D.D., Bai, R., 1999. Interfacial shapes in the steady flow of a highly viscous dispersed phase. In: Wei, S. (Ed.), Fluid Dynamics at Interfaces. Cambridge University Press.

Joseph, D.D., Renardy, Y.Y., 1993. Fundamentals of Two-Fluid Dynamics. Springer-Verlag, New York.

Joseph, D.D., Bai, R., Mata, C., Surry, K., Grant, C., 1999. Self-lubricated transport of bitumen froth. J. Fluid Mech. (in press).

Keil, O.M., 1968. US Patent 3,378,047.

Liti, H., 1982. A theory of capsule liftoff in pipeline. J. Pipelines 2, 23–33.

Looman, M.D., 1916. US Patent No. 1,192,438.

Neiman, O., 1986. Froth pipelining tests. Syncrude Can. Res. Dev. Prog. Rep. 15 (1), 373–407.

Oliemans, R.V.A., Ooms, G., 1986. Core-annular flow of oil and water through a pipeline. In: Hewitt, G.F., Delhaye, J.M., Zuber, N. (Eds.), Multiphase Science and Technology, Vol. 2. Hemisphere Publishing Corporation.

Oliemans, R.V.A., Ooms, G., Wu, H.L., Duÿvestin, A., 1985. Core-annular flow of oil/water flow: the turbulent-lubricating model and measurements in a 2 in. pipe loop. Presented at the Middle East Oil Technical Conf. and Exhibition, Bahrain, March 11–14, 1985. Soc. Pet. Eng.

Ooms, G., Segal, A., Van der Wees, A.J., Meerhoff, R., Oliemans, R.V.A., 1984. A theoretical model for core-annular flow of a very viscous oil core and a water annulus through a horizontal pipe. Int. J. Mult. Flow 10, 41–60.

Patankar, S.V., 1980. Numerical Heat Transfer and Fluid Flow. Hemisphere Publishing Corporation.

Preziosi, L., Chen, K., Joseph, D.D., 1989. Lubricated pipelining: stability of core-annular flow. J. Fluid Mech. 201, 323–356.

Russell, T.W.F., Charles, M.E., 1959. The effect of the less viscous liquid in the laminar flow of two immiscible liquids. Can. J. Chem. Eng. 39, 18–24.

Russell, T.W.F., Hodgson, G.W., Govier, G.W., 1959. Horizontal pipeline flow of mixtures of oil and water. Can. J. Chem. Eng. 37, 9.

Stein, M.H., 1978. Concentric annular oil/water flow. Ph.D. thesis, Pursue University.